异厚度铝合金薄板激光拼焊温度场数值模拟

余淑荣[1,2]， 熊进辉[1]， 樊 丁[2]，陈剑虹[1,2]
（1. 兰州理工大学 有色金属合金及加工教育部重点实验室，兰州 730050；
2. 兰州理工大学 甘肃省有色金属新材料省部共建国家重点实验室，兰州 730050）

余淑荣

摘 要：利用 ANSYS 软件对异厚度铝合金激光拼焊的温度场进行三维瞬态有限元分析。为了提高计算精度和效率，采用过渡网格划分形式划分网格以保证焊缝处网格足够细小。选取高斯函数分布的热源模型，利用 ANSYS 软件的 APDL 语言编写程序实现移动热源的加载。在模拟中既考虑一般激光焊接中材料热物理性能参数的温度相关性、熔化潜热、边界条件、等离子体、熔池对流、保护气体等对温度场的影响，又考虑异厚度铝合金激光拼焊的特性。利用高温热电偶检测异厚度铝合金激光拼焊过程中的温度场，将模拟值与实测值进行对比分析，结果表明，模拟值与实测值吻合良好。

关键词：铝合金；激光拼焊；异厚度；温度场；数值模拟
中图分类号：TG115.28 文献标识码：A 文章编号：0253－360X(2007)05－017－04

0 序 言

目前国际上对于交通工具如汽车、火车等的开发研究正朝着高效能、低能耗、低排放方向发展。剪裁拼焊板(tailored welded blanks)是近年来发展起来的一种新技术，激光剪裁拼焊板是将不同材质、不同厚度的板料经剪裁后，用激光焊接拼成各种坯板，然后整体冲压成形的一种加工工艺。剪裁拼焊钢板在汽车工业中的使用，有效地节省了材料，降低了车体重量，从而获得了很大的经济效益。国内外对铝合金剪裁拼焊板的研究是一个前沿热点[1]，并且正在逐步应用于交通工具。

激光焊接是一个快速而不均匀的热循环过程，焊缝附近出现很大的温度梯度，在焊后的结构中也会出现由温度梯度造成的不同程度的残余应力和变形，这些都成为影响焊接结构质量和使用性能的重要因素。所以，在异厚度铝合金激光拼焊工艺试验的基础上，用有限元方法对异厚度铝合金激光拼焊过程的温度场进行数值模拟，为模拟应力应变场做准备，对于优化焊接工艺参数，控制与预测焊接残余应力与变形，得到综合性能优良的铝合金拼焊板有很深刻的意义。

自从 1973 年 Swift Hook 和 Gick[2] 开始对激光焊温度场进行研究以来，激光焊接热效应过程数值模拟已经历了 30 多年的发展历史。目前，国内外的研究[3－5]主要集中在分析激光焊接热源模型、小孔模型、温度场、熔池行为、残余应力及变形等方面，但是针对异厚度铝合金激光拼焊过程的数值模拟还少见报道。

1 有限元分析模拟过程

1.1 有限元模型的建立及网格划分

试件尺寸分别为250 mm × 100 mm × 2 mm，250 mm×100 mm×1 mm，材料为铝合金 5A06。建立三维有限元实体模型，选择三维热分析单元 SOLID70。为了节省计算时间，提高计算效率，减少不必要的计算量，截取原试件中关键区域焊缝附近一小块建立有限元模型，有限元模型尺寸为25 mm× 10 mm× 1 mm，25 mm×10 mm×0.5 mm。采用有利于节省计算时间的一种特殊网格划分，远离焊缝位置的地方，由于温度变化不明显，温度梯度小，所以采用比较大的网格尺寸，在焊缝中心位置附近，温度场变化剧烈，需要采用较细密的网格划分，有限元网格共生成16 600个单元，19 910个节点，对接中心处最小网格尺寸0.2 mm，有限元网格划分如图 1 所示。

收稿日期：2006－06－02
基金项目：国家重大项目前期预研项目(2004CCA04900)；教育部“春晖计划”基金资助项目(Z2004－1－62008)；甘肃省自然基金资助项目(3ZS041－A25－031)

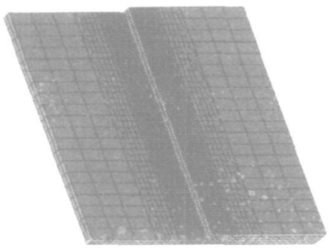

图 1 有限元网格划分

Fig. 1 Finite element mesh

1.2 热源模型的选取

对于薄板激光焊接，一般为传导焊机制。激光传导焊接的温度场计算，一般采取与电弧焊类似的处理办法，把热源看成点热源或二维面热源处理。面热源的能量密度分布为高斯分布[6]，其函数表达式为

$$q(r)=q_{\mathrm{m}}\exp\left(-\frac{3r^2}{R^2}\right), \tag{1}$$

式中：q_{m} 为加热斑点中心最大热流密度；R 为有效加热半径；r 为 A 点离电弧加热斑点中心的距离。由于高斯分布曲线在无限远处才趋近于零，因此对于高斯分布曲线，$q(r)\leqslant 0.05q_{\mathrm{m}}$ 可以忽略，按此推算出的有效加热半径 $R=0.6$ mm。在移动的热源中，$q_{\mathrm{m}}=3Q/\pi R^2$。

1.3 材料物理性能参数的选取

金属材料的物理性能参数如比热容、导热系数、弹性模量、屈服应力等一般都随温度的变化而变化。当温度变化范围不大时，可采用材料物理性能参数的平均值进行计算。但焊接过程中，焊件局部加热到很高的温度，整个焊件温度变化十分剧烈，如果不考虑材料的物理性能参数随温度的变化，那么计算结果一定会有很大的偏差。所以在焊接温度场的模拟计算中一定要给定材料的各项物理性能参数随温度的变化值。由文献[7]可以获得材料在部分温度点上的物理性能，通过插值法与外推法可以获得更高温度条件下的物理性能参数。

1.4 边界条件的处理

焊件的边界由于与外界存在温度差而与周围介质换热，其中包括对流和辐射换热。试验表明，在焊接时热能的损失主要通过辐射，而对流作用相对较小。温度越高则辐射换热作用越强烈。一般辐射与对流换热计算方式不同。为了计算方便，考虑总的换热系数。这样，因边界换热而损失的热能可表示为

$$q_0=\beta(T-T_0), \tag{2}$$

式中：T 为焊件表面温度；T_0 为周围介质温度；β 为表面换热系数，$\beta=\beta_{\mathrm{c}}+\beta_{\mathrm{e}}$；$\beta_{\mathrm{c}}$ 为对流换热系数；β_{e} 为辐射换热系数。

采用给实体模型表面覆盖三维表面效应单元 SURF152，在表面效应单元上施加对流边界条件。考虑保护气体的影响，上下表面，特别是对接面靠近焊缝附近处保护气体影响大，气体流速快，对流换热系数高；远离焊缝处保护气体影响小，气体流速慢，对流换热系数小；下端面附近保护气体影响很小，所以只考虑常温下与空气对流；上端面与左右端面是截取原试件的截面，但已经远离焊缝区域，如果只考虑与空气对流，则不能完全反映这三个方面的真实导热情况，所以采用适当提高这三个面上对流系数的方法，以近似该处的实际导热情况。由于辐射的计算与对流不同，且是 4 次方的非线性关系，容易使计算结果不收敛，所以采用适当提高对流系数的方法考虑辐射的影响。

1.5 相变潜热的影响

焊接过程中，母材熔化时，由固态变为液态，要吸收能量，反之熔池凝固时由液态变成固态，要放出热量，所以在计算温度场时，要考虑熔池相变潜热对温度场的影响。否则计算结果会有较大偏差。对于固态相变，由于其潜热一般比固液相变潜热小很多，通常将其忽略。采用比热突变法考虑相变潜热的影响，即在熔化范围内，给予比热一个适当的突变值，可按以下两式计算，即

$$C_{\mathrm{e}}=\Delta Q/\Delta T, \tag{3}$$

$$C_{\mathrm{p}}=C_{\mathrm{e}}+C, \tag{4}$$

式中：C 为不考虑潜热时的比热；C_{e} 为等效比热；ΔT 为凝固温度区间；ΔQ 为潜热。

1.6 光致等离子体和熔池对流的影响

在传导焊接中，没有小孔产生，等离子体处于工件表面上方，对激光束产生反射和折射，造成激光加工有效能量的损失，在模型中应适当减小激光束的效率系数来考虑此影响。

熔池对流对温度场的影响，在焊接速度比较快的情况下是不可忽略的，通过增加有效液体热传导率来近似考虑对流的增强，即适当提高熔点温度以上的导热系数近似考虑熔池对流的影响。

1.7 异厚度铝合金薄板激光拼焊特点的影响

异厚度拼焊时，试件的装夹比较困难，由于工装夹具的偏差造成对接间隙过大、错边、对中性差等会产生漏光现象，使激光有效能量有所损失，根据装夹情况适当调整激光有效吸收系数，以考虑此影响。

由于拼焊厚度不同，激光束应首先与厚板作用，厚板应首先熔化，但是由于激光传播的速度非常快，远快于金属的熔化速度，所以可以认为薄厚两板是同时熔化的。材料对激光的吸收效率与材料表面温

度与状态密切相关，当认为薄厚两板同时熔化时，即两板的表面状态同时变化，表面温度同时达到熔化温度。因此，在考虑薄厚两板的材料对激光的吸收率时，可以认为薄厚两板是一致的。

由于拼焊厚度不同，同一激光束落在两板上的光斑应该不同，但是对于高质量的激光光束，在焦点附近都有一定的焦深，即在焦点距离上下，光斑直径大小是一致的。因此，采用的离焦量较小时，可以忽略此影响，但是当离焦量较大时，不能忽略薄厚两板光斑大小的不同，应根据实际情况，增大或缩小薄板上光斑直径的大小。

2　模拟结果与分析

当激光入射功率 $P_0=1\ 500$ W，焊接速度 $v=1.0$ mm/s，离焦量为 0 时，有效作用半径0.6 mm不同时刻的整体温度场模拟结果如图 2 所示。由图可见，移动的激光热源经过一定时间后，焊件上形成了准稳

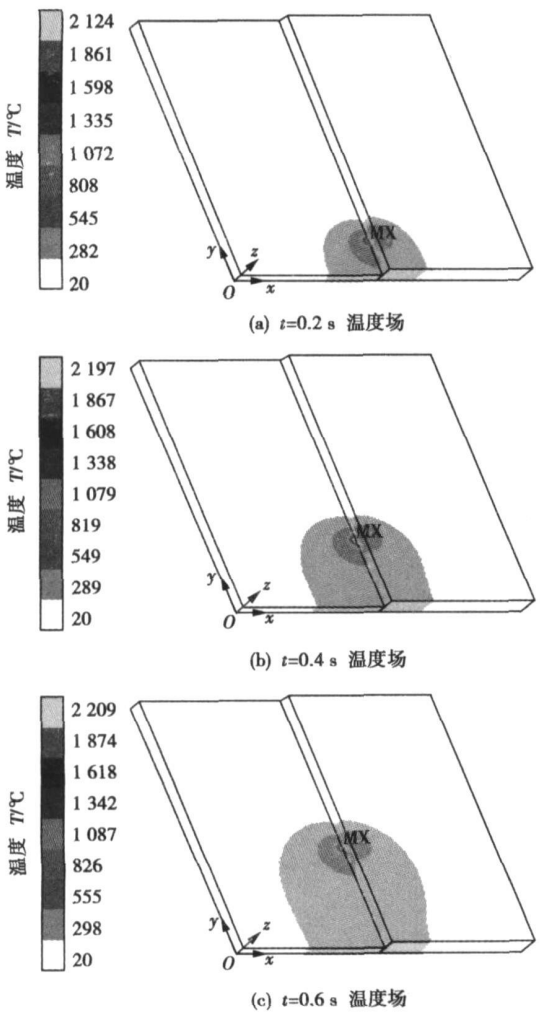

图 2　不同时刻的温度场分布图

Fig. 2　Temperature distribution at different time

定温度场，这时焊件上各点温度虽然随时间而变化，但各点以固定的温度跟随热源移动，也就是说，温度场与热源以同样的速度跟踪。

当薄厚两板上光斑分布相同、所加热流密度相同时，可以明显看到薄板上温度场范围比厚板大，熔池尺寸比厚板稍大，薄板熔化范围比厚板大。薄厚两板上对应点的温度，薄板高于厚板，这是由于在输入相同热量时，薄板用于加热的体积小而升温高的缘故。板件中心等距三个点的热循环曲线如图 3 所示，它表示了焊缝中心的加热、冷却速度以及所能达到的峰值温度，峰值温度都在2 000 ℃以上，远高于材料的熔点。由图可见，对接中心点的温度梯度非常高，热源经过时，温度迅速上升，平均温度梯度可达500 ℃/s以上。由于铝合金的导热系数较大，所以热源经过后，其降温速度也非常快。

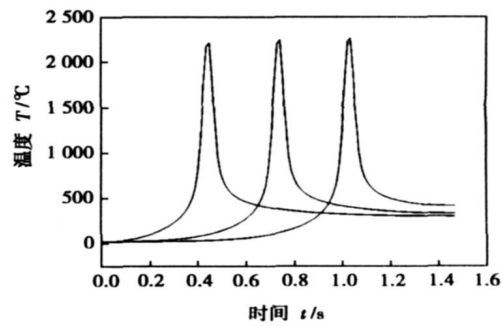

图 3　板件中心不同点的热循环曲线

Fig. 3　Thermal cycle curve of plate center at different points

3　模拟结果与试验结果的对比

在工件表面依次取坐标点 A，B 两点，两点距对接中心都为3 mm，用于试验测试结果与模拟结果的比较，取点位置如图 4 所示。

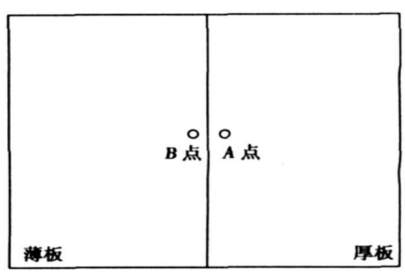

图 4　板中的测量点

Fig. 4　Experiment points in plate

试验与模拟采用相同的焊接工艺(激光功率1.5 kW,焊接速度1.0 m/min),利用高温热电偶进行焊接热循环测定,由于测量值是非连续的,为了更好的对比每个测量时间的测量值和模拟值,模拟值也按测量时间取非连续的点。试验测得各点的热循环曲线与模拟热循环曲线对比如图5所示。

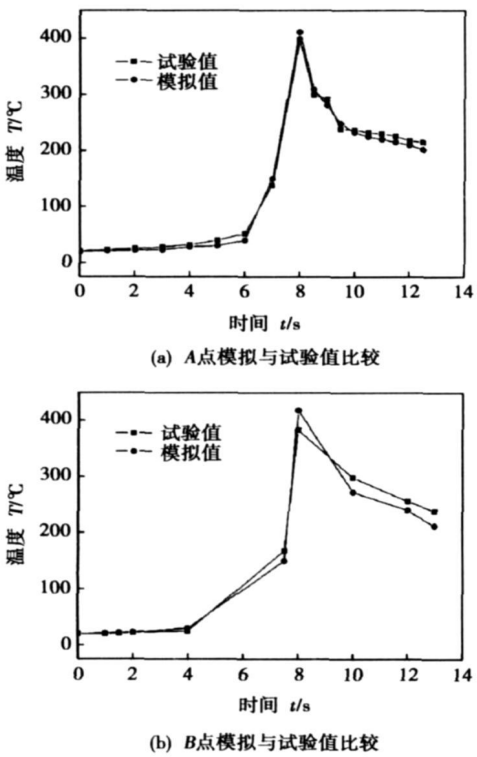

(a) A点模拟与试验值比较

(b) B点模拟与试验值比较

图5 模拟值与实测值的比较

Fig. 5 Comparison between experiment value and simulation value

从图中可以看出,两者吻合较好,但存在一定的偏差,特别是在薄板测量时,误差比较大。误差主要来源于三个方面:一是测量试验的不精确性;二是激光焊接过程影响因素非常多,而且重复性差;三是建立的数学物理模型还需进一步完善。

4 结 论

(1)激光作用一定时间后,焊件上形成了准稳态温度场。

(2)薄厚两板温度场存在差异,薄板温度场范围较大,熔池尺寸比厚板稍大,薄板熔化范围比厚板大。

(3)将有限元的模拟结果与实测结果进行对比分析,结果显示模拟值与实测值吻合良好。

(4)通过对温度场的准确模拟,建立准确的有限元模型,为模拟应力应变场做好准备。

参考文献:

[1] 余淑荣,樊 丁,陈剑虹,等. 铝合金激光剪裁拼焊板技术[C] // 2003 汽车焊接国际论坛论文集. 上海:中国机械工程学会,2003:199—303.

[2] Swift Hook, Gick. Penetration welding with laser[J]. Welding Journal, 1973, 52(11): 492—498.

[3] 薛忠明,顾 兰,张彦华. 激光焊接温度场数值模拟[J]. 焊接学报,2003,24(2):79—80.

[4] 韩国明,李建强,闫青亮. 不锈钢激光焊温度场的建模与仿真[J]. 焊接学报,2006,27(3):105—108.

[5] Wei Shian. Three-dimensional analytical temperature field and its application to solidification characteristics in high-of Low-power-density-beam welding[J]. Heat Mass Transfer, 1997, 40(10): 2283—2292.

[6] 张文钺. 焊接传热学[M]. 北京:机械工业出版社,1989.

[7] 田荣璋,王祝堂. 铝合金及其加工手册[M]. 长沙:中南大学出版社,2000.

作者简介:余淑荣,女,1968 年出生,副教授,博士研究生。主要研究方向为材料的激光加工及数值模拟。发表论文 10 余篇。

Email: yushur@lut.cn

MAIN TOPICS, ABSTRACTS & KEY WORDS

Simulation of Al-MIG weld pool width control by nine-point controller FAN Ding[1,2], LI Jianjun[1], SHI Yu[1], GAO Yuan[2] (1. Key Laboratory of Advanced Processing Technology for Non-ferrous Materials, The Ministry of Education, Lanzhou University of Technology, Lanzhou 730050, China; 2. State Key Laboratory of Gansu Advanced New Non-ferrous Metal Materials, Lanzhou University of Technology, Lanzhou 730050, China). p1—4

Abstract: Considering the characteristics of aluminum alloy MIG welding process, nine-point controller was developed to control weld pool width. The structure and the principle of nine-point controller were analyzed. Based on the mathematic model of step response between pulse current and weld pool width, the simulations on three controlles of PID, fuzzy and nine-point controller used to control aluminum alloy MIG weld pool width were studied. The simulation results show that nine-point controller not only has the best stability and robust than PID and fuzzy controller, but also assure the control accuracy and provides the theoretical basis to realize the intelligent control for aluminum alloy pulsed MIG welding process.

Key words: aluminum alloy; metal inert gas welding; nine-point controller; intelligent control; simulation

Effect of brazing residual stress on creep for stainless steel plate-fin structure JIANG Wenchun, GONG Jianming, TU Shandong, CHEN Hu (College of Mechanical and Power Engineering, Nanjing University of Technology, Nanjing 210009, China). p5—8, 12

Abstract: The effect of residual stress on creep for microminiaturized nickel base brazed stainless steel plate-fin structure was analyzed by finite element method with ABAQUS code. The results show that because of mismatch of mechanical properties between filler metal and base metal, the welding residual stress was generated inevitably, which has great influence on the creep deformation and life. The residual stress can not be ignored in the strength design and should be controlled during the manufacture of plate-fin structure. The stress and strain is concentrated in the fillet where the creep crack will initiate, propagate and result in the failure. The strain and stress in plate is larger than that in fin, so the cracking susceptibility of plate is lager than that of fin. The present work provides a reference for strength design at high temperature for plate-fin structure.

Key words: stainless steel plate-fin structure; brazing residual stress; creep; finite element

Effect of processinig parameters on sheet-tube indirect spot welding process YANG Honggang, ZHANG Yansong, CHEN Guanlong (School of Mechanical Engineering, Shanghai Jiaotong University, Shanghai 200030, China). p9—12

Abstract: In sheet-tube indirect spot welding, it is difficult to assure welding quality because the welding deformation is too large. The expansion and welding deformation were investigated and the influence of different welding parameters (welding current, electrode force and welding time) on indirect spot welding process was analyzed through electrode displacement. The experiment result shows that the course of the expansion and welding deformation are coupled to each other in the welding stage; in the holding stage, welding deformation gets larger under the ailion of applied electrode force. Maximum welding deformation of sheet-tube indirect spot welding process is almost linear with electrode force and input welding energy. Ladder-type occurs in the electrode displacement curve when the expulsion happens, so the expulsion can be judged according to the slope coefficient of electrode displacement. The result provides a theoretical guidance for on-line monitoning and control of welding quality in sheet-tube indirect spot welding process.

Key words: indirect spot welding; electrode displacement; welding deformation

Pure copper coating deposited by automatic plasma welding with melting strip electrode technology WANG Kehong, LI Jianyong, JI Dayuan, ZHANG Deku (Department of Material Science and Engineering, Nanjing University Science and Technology, Nanjing 210094, China). p13—16

Abstract: For tubular workpiece surface deposited by Cu, the process of deposition by automatic plasma welding with melting strip electrode was designed and researched. The Cu strip electrode enters the welding region with the passive automatic feed-in manner. The plasma arc burns between the tungsten, and copper strip and the protective agent is blown into the welding region. The plasma arc makes the copper strip melt, and the Cu deposited layer was formed on the base metal surface of steel. The welding process is stable and the weld appearance is excellent. The detected results show that the deposited layer of of pure copper with 1—6 mm thickness can be gotten. The pure copper and the base metal can be welded together without the base metal being molten. The shear strength exceeds 150 MPa, which is greater than the strength of Cu layer. The bonding quality is excellent and there is no welding defects such as gas pore, incomplete fusion and slag inclusion. The SEM and EDAX results show that metallurgical bonding by diffusion is formed between the deposited pure copper layer and the base metal. And within the distance of 10—30 μm from the side of the deposited copper layer interface, the content of Fe decreases to less than 1%.

Key words: deposited welding; melting strip electrode; plasma arc; copper strip; automatic welding

Numerical simulation on temperature field in laser welding of thin aluminum alloy plate with different thickness YU Shurong[1,2], XIONG Jinhui[1], FAN Ding[1,2], CHEN Jianhong[1,2] (1. Key Laboratory of Non-ferrous Metal Alloys, The Ministry of

Education, Lanzhou University of Technology, Lanzhou 730050, China; 2. State Key Laboratory of Advanced Non-ferrous Metal Materials, Lanzhou University of Technology, Lanzhou 730050, China). p17—20

Abstract: By using ANSYS, the 3D temperature field of laser welding for aluminum alloy of different thickness were simulated. In order to improve solution accuracy and efficiency, transition mesh and Gauss function heat source model were used, and APDL in ANSYS was used to compile program to realize the load of moving heat source. The effects of temperature-dependence material parameters and potential heat, boundary conditions, plasma, convection in molten pool and characteristics of different thickness were considered in the model. Using high-temperature thermocouple, the temperature was measured. It is shown that the simulation results are in accordance with the experimental results.

Key words: aluminum alloy; laser welding; different thickness; temperature field; numerical simulation

Effects of laser soldering speed on mechanical properties of SOP micro-joints XUE Songbai, HUANG Xiang, WU Yuxiu, HAN Zongjie (College of Materials Science and Technology, Nanjing University of Aeronautics and Astronautics, Nanjing 210016, China). p21—24

Abstract: SOP(small outline package) devices were soldered by diode-laser soldering and IR reflow soldering method respectively and the tensile strengths of soldered joints were measured by Micro-joints Tester(STR-1000), and the effects of laser soldering speed on mechanical properties of SOP micro-joints were studied and the characteristics of fracture microstructures of micro-joints were also analyzed by SEM. The results indicate that the tensile strength of soldered joints is influenced remarkably by laser soldering speed, and the mechanical properties of the joints soldered with Sn—Ag—Cu solder are more sensitive to soldering speed than that with Sn—Pb solder, and there is an optimal speed of laser soldering according to the best mechanical property. There are some micropores and shallow dimples when the speed is lower, which is called micropore aggregation fracture. There are plenty of dimples in the fracture and some sidesteps in the local zone of the fracture when the speed is higher, which the fracture includes dimple and cleavage fracture, and when the speed is moderate, there are lots of big and deep dimples in the fracture, which is the ductile fracture.

Key words: laser soldering; soldering speed; mechanical property

Brazing/hot-rolling technique for preparation of stainless steel/carbon steel cladding plate ZU Guoyin, YU Jiuming, WEN Jinglin (School of Materials and Metallurgy, Northeastern University, Shenyang 110004, China). p25—28

Abstract: Aiming at the main problems in the explosion-rolling bonding process of stainless steel/carbon steel cladding plate, a new technique of brazing/hot-rolling method was put forward, and the effect of main process parameter on the bonding strength of brazing cladding plate was studied, and the bonding mechanics of hot-rolling cladding plate was analyzed, and the main mechanical properties of cladding plate was tested. The results showed that an effective brazing bonding can be gotten by using home-made silver base solder. The oplimized processing parameters are as follows: brazing temperature is 755—770 ℃ and holding time is 2.5—3 min. Soldered layer shows good plasticity during hot-rolling process. When the deformation rate was 40%, there was no fracture and lamination in soldered layer after rolling. Metallic bonding formed between the soldered layer and the base metal, and the bonding strength of the stainless steel/soldered interface obviously increased, and the shear strength of cladding plate after hot-rolling can be reached 342.6 MPa.

Key words: stainless steel/carbon steel cladding plate; brazing; solder; hot-rolling; deformation rate

Effects of electrode pitting morphology on resistance spot welding of aluminum alloy CHANG Baohua[1], DU Dong[1], CHEN Qiang[1], Zhou Y[2]. (1. Department of Mechanical Engineering, Tsinghua University, Beijing 100084, China; 2. Department of Mechanical Engineering, University of Waterloo, Waterloo, Ontario, N2L 3G1, Canada). p29—32

Abstract: The effects of two types of electrode pitting morphologies, ring type and hole type on resistance spot welding of aluminum alloy 5182 were investigated by the combination of finite element analysis and physical modeling methods. Results showed that when using ring pitting electrode, the contact radius at faying surface is increased while the current distribution is not affected notably, and the nugget diameter is increased. When using hole pitting electrode, the contact radius at faying surface is increased further and the current density is decreased in the contact region. In addition, electric current does not flows through the central part of faying surface under such conditions, consequently, central part does not melt and only donut shape nugget is formed. Hole type pitting reduces the joint strength significantly, and its detrimental influence on joint quality is much greater than that of ring type pitting.

Key words: resistance spot welding; pitting; electrode degradation; aluminum alloys; finite element method

Influence of pin shape on weld transverse morphology in friction stir welding KE Liming[1,2], PAN Jiluan[1], XING Li[2], WANG Shanlin[2](1. Key Laboratory for Advanced Manufacturing by Materials Processing Technology, The Ministry of Education, Tsinghua University, Beijing 100084, China; 2. Department of Materials Science and Engineering, Nanchang Institute of Aero-Technology, Nanchang 330063, China). p33—37

Abstract: Friction stir welding was conducted by using four types of pin and copper foils, piled up with aluminum plate alternately, as a tracer material. The distribution feature of the tracer materials was observed after welding. The results showed that, the flow of the plasticized metal in the weld is influenced by the pin shopes, which results in the variety of the morphology of the weld. If the screw thread on the pin is counter-clockwise, the metal around the pin will move downwards, which drives the metal around the pin tip to move around and upwards. So the center of the nugget is located at the lower part of the tansverse weld section. If the screw thread